Semiconductor Optoelectronics
ISSN: 1001-5868

TWO MODE (DE-)MULTIPLEXERS BASED ON CASCADED MULTIMODE INTERFERENCE STRUCTURES USING SILICON WAVEGUIDES

The Duong Do[a], Van Hung Tran[a] , Trung Thanh Le[*,b]

[a]University of Transport and Communications (UTC), Hanoi, 1000000, Vietnam
[b*]International School (VNU-IS), Vietnam National University (VNU), Hanoi, 1000000, Vietnam. Email: thanh,le@vnu.edu.vn

Abstract:

We present a new design of a TE0 and TE1 mode division multiplexer and de-multiplexer based on cascaded multimode interference (MMI) structures using silicon waveguides. The new design uses only two multimode interference structures for ease of fabrication. The footprint of the device is about 6 µm x400µm, the mode conversion efficiency is about 99.6%. The device exhibits low insertion loss of - 0.1 dB and crosstalk better than 40.9 dB at the operating wavelength of 1550 nm. The proposed device can provide large fabrication tolerance of 500nm and 800nm for TE1 and TE0 and a high mode conversion efficiency of 96%-99.6%.

Keywords: Asymmetric directional coupler, mode division multiplexer, multimode interference, optical interconnects, silicon photonics.

1. Introduction

The rapid growth of data transmission and connectivity has led to the development of various technologies, including on-chip wavelength division multiplexing (WDM), advanced modulation formats, and mode division multiplexing (MDM) [1] [2]. The phase match condition between different modes can be disrupted by even slight variations in the waveguide width during fabrication, resulting in performance degradation [3]. To ensure optimal performance, it is recommended that fabrication errors are limited to 5 nm or less [4]. As data transmission volumes continue to grow rapidly, there is a need for innovative approaches to increase the capacity of optical communication systems [5]. To address this, various multiplexing techniques have been introduced, with wavelength division multiplexing (WDM) being the most widely used for many years [6]. However, the capacity of WDM networks that transmit data on a single mode and different wavelengths is reaching the theoretical Shannon limit. Additionally, the deployment of dense WDM networks requires multiple precise wavelength sources, leading to higher costs and energy consumption. Therefore, the use of WDM is limited by the need for multiple sources with precise wavelength tuning.

Integrated mode multiplexers are an essential component of on-chip MDM, which offers an additional degree of freedom to increase the transmission scalability [7]. These multiplexers are designed to be wavelength-insensitive and have high extinction ratios. Mode division

multiplexers (MDMs) and de-multiplexers play a crucial role in the design of optical communication systems, and are also among the most challenging components to design. To develop mode multiplexers, various materials are used. However, the silicon-on-insulator (SOI) multiplexer has gained significant attention due to its compatibility with complementary metal-oxide-semiconductor (CMOS) fabrication technology, compact size, and high performance [8] [9]. Consequently, there have been several reports on different types of SOI-based MDMs.

Several technologies [10] [11] have been investigated to develop integrated mode multiplexers, including Y-junctions, multimode interferometers, ring resonators, asymmetric directional couplers (ADC), meta-materials, inversed design, and pixelated waveguides [12]. Each of these technologies has its advantages and disadvantages in terms of performance, complexity, and cost. Y-junctions are widely used due to their simplicity and compatibility with standard fabrication processes. Multimode interferometers offer high extinction ratios and low loss, while ring resonators provide narrow bandwidths and compact device footprints. ADCs offer broad bandwidths and low crosstalk, while meta-materials and inversed design offer unique polarization and mode control. Pixelated waveguides are a relatively new technology that allows for precise mode manipulation and can be used to implement more complex mode multiplexers. Overall, each of these technologies has its strengths and can be used to address different design requirements for integrated mode multiplexers. Multiplexing techniques that rely on asymmetric directional couplers (ADCs) have certain drawbacks, such as large device footprints, complex and strict designs, and sensitivity to angles. Although adiabatic mode evolution-based devices have been reported for relatively high bandwidth operations, they often require a large length. In general, the main limitation of ADCs is their sensitivity to process variations, which can affect their performance. Additionally, ADCs typically have a limited operation wavelength or optical bandwidth, usually only a few tens of nanometers.

In this design, we present a new method for designing a TE0/TE1 mode multiplexer using only multimode interference (MMI) structures. This design offers several advantages, including good fabrication tolerance, ease of fabrication, low insertion loss, high crosstalk, and high bandwidth. The optical mode multiplexing device utilizes SOI waveguides due to their compatibility with CMOS technology.

2. Proposal of the new cascaded MMI structure

A schematic of the proposed two-mode multiplexer is shown in Figure 1. The device consists of two cascaded MMIs with length L1 and L2. The silicon waveguide with a height of 220nm is used. Using the numerical simulations (based on Finite Difference Method-FDM). for single mode operation of the input and output waveguides, the width of the waveguide is selected to be $W_a = 500nm$. To support two modes: the fundamental mode TE0 and the first order mode TE1, we choose the width of the input waveguide of $W_{in} = 2W_a = 1000nm$. The operating wavelength is around 1550nm.

The operating principle of the proposed two-mode multiplexer is as follows: Input signal is at input port consisting of two modes TE0 and TE1. The first MMI coupler (MMI 1) with a width W1 and length L1 is designed to separate the TE0 going out to the output port 1. The TE1 shall continue to go the next region (MMI 2). The next region with width W2 and L2

supporting multimode operation. We need to carefully design this region to get the mode TE1 at the output port 2. The input field can be expressed by [13]:

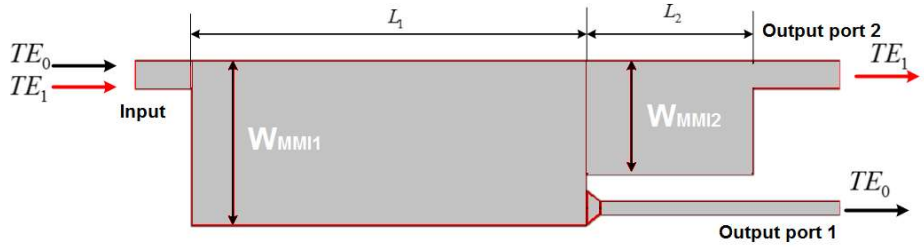

(a)

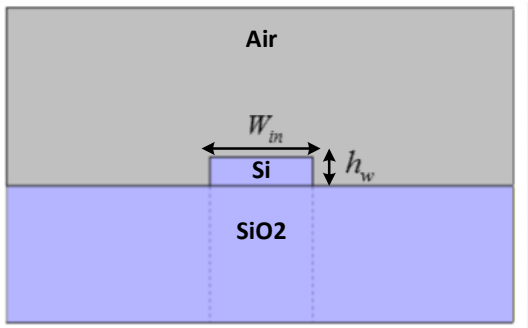

(b)

Figure 1. (a) Proposed two mode multiplexer and (b) cross-section view of the SOI waveguide

$$f_{in1}(x)=\sum_{i=0}^{M-1}c_iE_{1i}(x)=\sum_{i=0}^{M-1}c_i\,sin[\pi(i+1)\frac{x}{W_1}] \quad \text{for TE0 at the MMI 1} \tag{1}$$

$$f_{in2}(x)=\sum_{i=0}^{M-1}c_{2i}E_{2i}(x)=\sum_{i=0}^{M-1}c_{2i}\,sin[\pi(i+1)\frac{x}{W_2}] \quad \text{for TE1 at the MMI 2} \tag{2}$$

where for the field of TE0 is $E_{TE0}(x)=sin\frac{\pi x}{W_{in}}$ and the field of the TE1 is $E_{TE1}(x)=sin\frac{2\pi x}{W_{in}}$; the coefficient $c_{1i}=\frac{2}{W_1}\int_0^{W_1}f_{in1}(x)E_{1i}^*(x)dx$, $c_{2i}=\frac{2}{W_2}\int_0^{W_2}f_{in2}(x)E_{2i}^*(x)dx$. In this design, we use the general interference MMI for large distance between two output ports for reducing loss and device footprint [14]. The length of the MMI 1 is chosen to be $L_1=3L_\pi$ to get the output at output port 1 for TE0, where $L_\pi^{MMI1}=\frac{\pi}{\beta_0-\beta_1}$ is the beat length of the MMI 1, β_i is the propagation constants of the order mode i. As a result, the output signals at the port 1 with location x_1 and port 2 with location x_2 are [15]:

$$f_{out1}(x)=\sum_{i=0}^{M-1}f_{in1}(x-x_1)exp(j\varphi_1) \tag{3}$$

$$f_{out2}(x)=\sum_{i=0}^{M-1}f_{in2}(x-x_2)exp(j\varphi_2) \tag{4}$$

When two MMI structures with similar widths are connected, and most of the optical

power is coupled into the succeeding MMI with negligible loss, the optical power can be expressed by superimposing the second MMI propagation modes with nearly the same coefficients as in the first MMI region. At the position of z, it can be rewritten as:

$$f_{out2}(x)=\sum_{i=0}^{M-1} f_{in2}(x-x_2)\,exp\left[-j\pi i(i+2)\left(\frac{L_1}{L_\pi^{MMI1}}+\frac{z-L_1}{L_\pi^{MMI2}}\right)\right] \quad (5)$$

First of all, assume that the TE0 with recombination length $L_{TE0}(W_1)$, and the TE1 is recombination length $L_{TE1}(W_2)$. The aim of the design is to find out the optimal length:

$$L_1=L_{TE0}(W_1)=L_{TE1}(W_1)(1-\varepsilon) \text{ and } L_2=L_{TE1}(W_2)(1+\varepsilon) \quad (6)$$

Where ϵ is the length adjustment. Based on these analytical expressions, we use the Eigen-mode Expansion method (EME) and Beam propagation method (BPM) for numerical optimal design of the proposed device.

3. Simulation Results and Discussions

The field profiles of the fundamental mode TE0 and the first order mode TE1 of the input signals at input port with a width of 1000nm are presented in Figure 2.

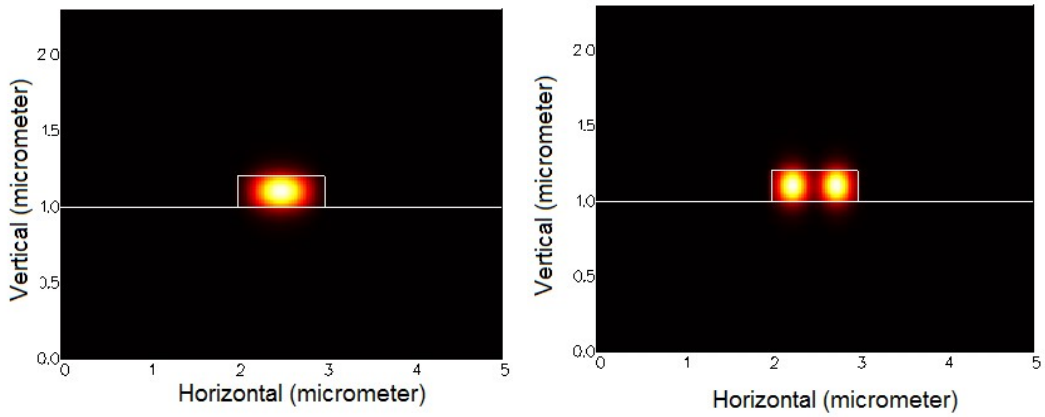

(a) (b)

Figure 2. Mode profile (a) fundamental mode TE0 and (b) first order mode TE1

First, we optimal design the first MMI (MMI1). We need to find out the optimal length using the numerical simulations around the analytical length of 273 μm calculated from the equation $L_1=3\frac{\pi}{\beta_0^{MMI1}-\beta_1^{MMI1}}$. Figure 3(a) presents the transmission at output port 1 and 2 for the excited input signal TE0. From this simulation, the optimal length of the MMI 1 is calculated to be $275.3\mu m$. At this optimal length, we excite the input signal with the TE1 mode. The transmission for TE1 mode input at different lengths of the MMI 2 is plotted in Figure 3(b). The optimal length of the MMI 2 is found to be 115.6 μm.

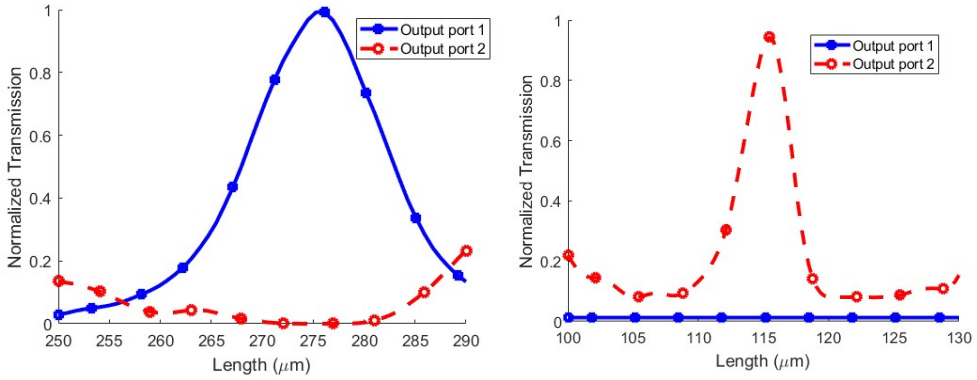

(a) (b)

Figure 3. Transmission at output port 1 and 2 with (a) TE0 and (b) TE1

To evaluate the performance of the proposed device, we calculate the mode conversion efficiency (MCE), insertion loss (IL) and mode crosstalk (CT) by the following equations [16]:

$$MCE = \frac{P_{TE0}}{P_{TE0} + P_{TE1}}, \text{IL}=10\log(\frac{P_{TE0}}{P_{TE1}}) \text{ and CT}=10\log(\frac{P_{TE0}}{P_{Undesired}}) \quad (7)$$

where P_{TE0}, P_{TE1} are normalized powers at port 1 and 2, $P_{Undesired}$ is the undesired power at port 1 (power of TE1 at port 1 while input is TE0 or power of TE0 at port 2 while input is TE1). The insertion losses at different length L1 and L2 are presented in Figure 4. We can see that the insertion loss at optimal length is about -0.1 dB compared with about around -2 ÷ -3dB in the literature. For TE0 mode, we find out the MCE of 99.6% and the crosstalk of 41.3dB at the optimal length. For TE1 mode, we have the MCE of 96% and the crosstalk of 40dB at the optimal length. As a result, the proposed device provide a good crosstalk compared with other research (with crosstalk from -10 to 30dB).

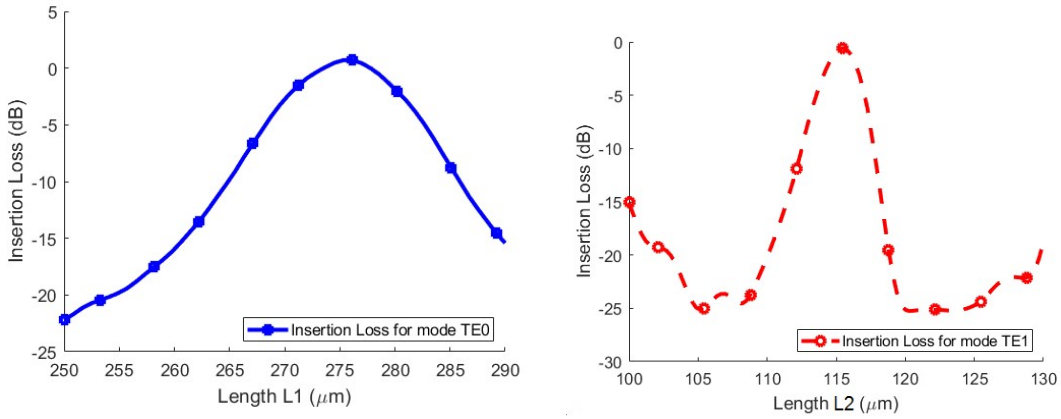

(a) (b)

Figure 4. Transmission at output port 1 and 2 with (a) TE0 and (b) TE1

Next, we consider the working operation of the proposed device at different wavelengths. The transmissions at different wavelengths at port 1 and 2 for input signal TE0 and TE1 are shown in Figure 5. The simulations showed that a -3dB bandwidth of 80nm for TE0 and 40nm for TE1 can be obtained. The achieved bandwidth is quite high compared with the published research at 30-100nm.

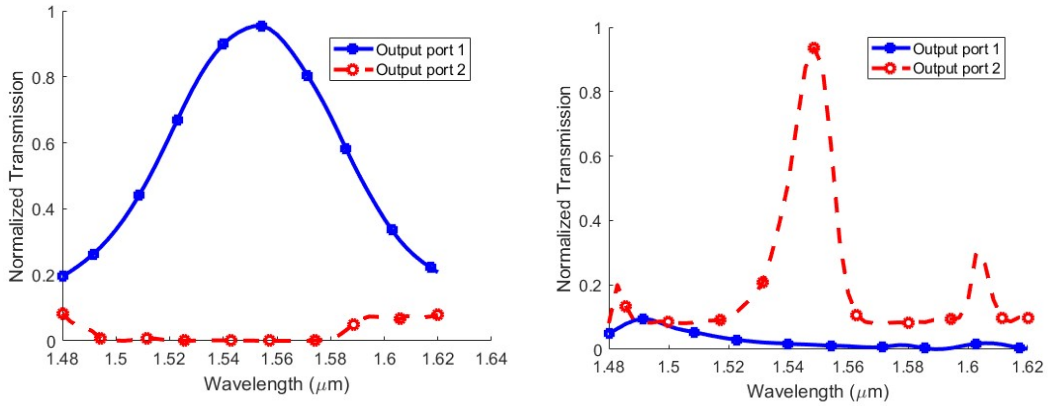

(a) (b)

Figure 5. Transmission at different operating wavelengths for output port 1 and 2 (a) TE0, (b) TE1

To estimate the fabrication tolerance of the (de)-multiplexer, we studied the TE0-TE1 conversion loss dependence on fabrication deviations for the lengths of MMI 1 and MM2. To study the effect of fabrication variability, the length of MMI 1 ($L1 \pm \Delta L_1$) and length of MMI 2 ($L_2 \pm \Delta L_2$) are changed, where ΔL_1, ΔL_2 are the length deviations due to fabrication error. Figure 6 presents the simulation results of the transmission at different ΔL_1, ΔL_2. The simulations shows that large fabrication tolerance of 800nm and 500nm for MMI 1 and MMI 2, respectively for a reduction of 10% in powers. For silicon photonics, CMOS technology is used. The process deviation of ± 5 nm is feasible in practice. Therefore, the proposed device can get a very high fabrication tolerance. This can provide a flexible fabrication process.

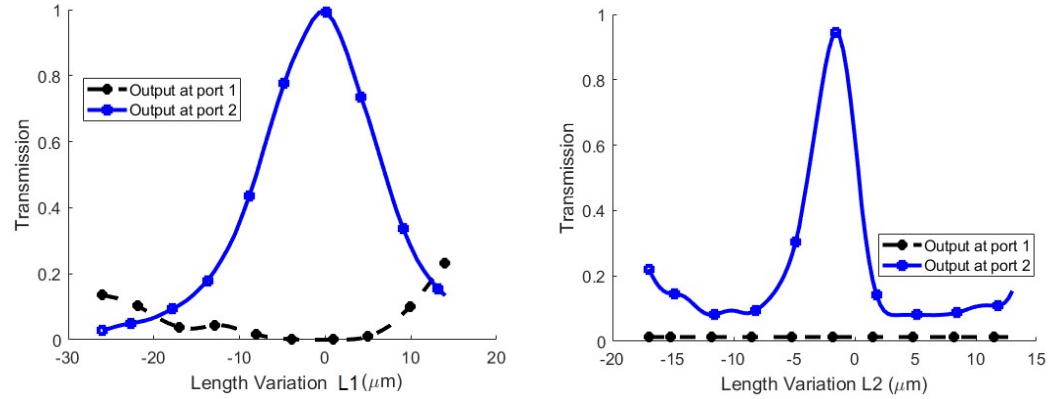

(a) (b)

Figure 6. Fabrication tolerance analysis for (a) TE0 and (b) TE1

Finally, we simulate the field propagation through the device for input signal TE0 and TE1 as shown in Figure 7. The length and width of the whole structure are at the optimal lengths, which are calculated from the above analysis.

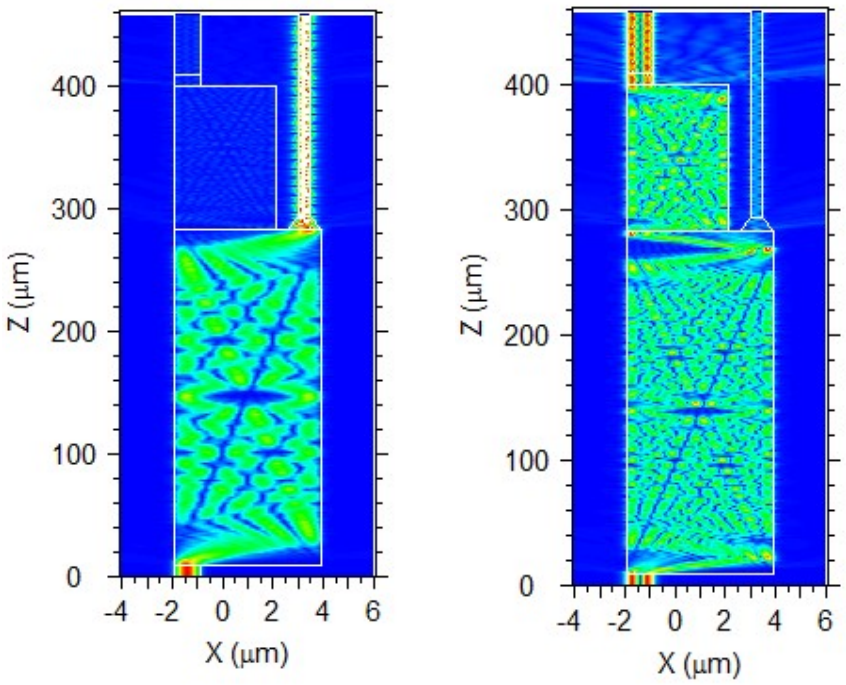

(a) (b)

Figure 7. BPM simulation results for the proposed device with input signal of (a) TE0 and (b) TE1

4. Conclusions

We have presented a new design of a two mode multiplexer based on only multimode interference structures. The SOI waveguide is used for the whole design. The proposed device can provide a small footprint of 6 µm x400µm, a small insertion loss of -0.1dB, crosstalk of 40-41.6dB for TE1 and TE0, large fabrication tolerance of 500nm and 800nm for TE1 and TE0 and a high mode conversion efficiency of 96%-99.6%. The proposed device also has advantage of ease of fabrication due to the cascaded MMIs. The proposed device can be useful for MDM systems and optical interconnects. To have a higher order modes coupled to the systems, the device can be extend to the higher order mode multiplexing.

Acknowledgement

This research is funded by Vietnam National Foundation for Science and Technology Development (NAFOSTED) under grant number 103.03-2018.354.

References

[1] B. Ni and J. Xiao, "Compact and broadband silicon-based mode-division (de)multiplexer using an asymmetrical directional coupler," *Optics Communications,* vol. 451, pp. 141-146, 2019/11/15/ 2019, doi: https://doi.org/10.1016/j.optcom.2019.06.043.

[2] J. Cui *et al.*, "Design of a highly mode-selective photonic lantern for IM/DD MDM transmission," *Optics Communications,* p. 129550, 2023/04/29/ 2023, doi: https://doi.org/10.1016/j.optcom.2023.129550.

[3] H. Xu, G. Zhang, K. R. Mojaver, and O. Liboiron-Ladouceur, "Broadband polarization/mode insensitive 3-dB optical coupler for silicon photonic switches," *Optics Express,* vol. 31, no. 9, pp. 14068-14080, 2023/04/24 2023, doi: 10.1364/OE.486454.

[4] B. Paredes, Z. Mohammed, J. Villegas, and M. Rasras, "Dual-Band (O & C-Bands) Two-Mode Multiplexer on the SOI Platform," *IEEE Photonics Journal,* vol. 13, no. 3, pp. 1-9, 2021, doi: 10.1109/JPHOT.2021.3075292.

[5] H. Shu, B. Shen, Q. Deng, M. Jin, X. Wang, and Z. Zhou, "A Design Guideline for Mode (DE) Multiplexer Based on Integrated Tapered Asymmetric Directional Coupler," *IEEE Photonics Journal,* vol. 11, no. 5, pp. 1-12, 2019, doi: 10.1109/JPHOT.2019.2941742.

[6] K. Zou *et al.*, "High-capacity free-space optical communications using wavelength- and mode-division-multiplexing in the mid-infrared region," *Nature Communications,* vol. 13, no. 1, p. 7662, 2022/12/10 2022, doi: 10.1038/s41467-022-35327-w.

[7] Y. Gao, D. Zhang, Y. Xu, X. Fan, F. Wang, and X. Sun, "Ultra-broadband polymer E00/E10 mode converter," *Optics Communications,* vol. 508, p. 127715, 2022/04/01/ 2022, doi: https://doi.org/10.1016/j.optcom.2021.127715.

[8] Y. Liu, S. Wang, J. Wang, X. Li, M. Yu, and Y. Cai, "Silicon photonic transceivers in the field of optical communication," *Nano Communication Networks,* vol. 31, p. 100379, 2022/03/01/ 2022, doi: https://doi.org/10.1016/j.nancom.2021.100379.

[9] X. Fu, J. Niu, Y. Huo, S. Yang, and L. Yang, "Polarization-Independent Reconfigurable WDM-MDM Hybrid Multiplexer on Silicon Photonics Platform," *IEEE Photonics Technology Letters,* vol. 35, no. 8, pp. 438-441, 2023, doi: 10.1109/LPT.2023.3253931.

[10] X. Wang *et al.*, "Ultra-compact silicon mode (de)multiplexer based on directional couplers with subwavelength sidewall corrugations," *Optics Letters,* vol. 47, no. 9, pp. 2198-2201, 2022/05/01 2022, doi: 10.1364/OL.449493.

[11] P.-C. Kuo *et al.*, "Design Consideration, Numerical and Experimental Analyses of Mode-Division-Multiplexed (MDM) Silicon Photonics Integrated Circuit with Sharp Bends," *Sensors*, vol. 23, no. 6*,* doi: 10.3390/s23062965.

[12] H. Xie *et al.*, "Highly Compact and Efficient Four-Mode Multiplexer Based on Pixelated Waveguides," *IEEE Photonics Technology Letters,* vol. 32, no. 3, pp. 166-169, 2020, doi: 10.1109/LPT.2020.2964308.

[13] T.-T. L. a. D.-T. Le, "High FSR and Critical Coupling Control of Microring Resonator Based on Graphene-Silicon Multimode Waveguides," in *Electromagnetic Propagation and Waveguides in Photonics and Microwave Engineering*, P. Steglich Ed.: IntechOpen, DOI: 10.5772/intechopen.92210, 2020.

[14] T.-T. Le, *Multimode Interference Structures for Photonic Signal Processing*. LAP Lambert Academic Publishing, 2010.

[15] M. Bachmann, P. A. Besse, and H. Melchior, "General self-imaging properties in N x N multimode interference couplers including phase relations," *Appl. Opt.,* vol. 33, no. 18, pp. 3905-, 1994.

[16] K. Mehrabi and A. Zarifkar, "Ultracompact and broadband asymmetric directional-coupler-based mode division (de)multiplexer," *J. Opt. Soc. Am. B,* vol. 36, no. 7, pp. 1907-1913, 2019/07/01 2019, doi: 10.1364/JOSAB.36.001907.